Elasticity of single-crystal methane hydrate at high pressure

Hiroyasu Shimizu,[1,2] Tatsuya Kumazaki,[2] Tetsuji Kume,[1] and Shigeo Sasaki[1,2]

[1]*Department of Electronics, Gifu University, 1-1 Yanagido, Gifu 501-1193, Japan*

[2]*Environmental and Renewable Energy Systems, Graduate School of Engineering, Gifu University, 1-1 Yanagido, Gifu 501-1193, Japan*

(Received 9 August 2001; published 14 May 2002)

By using *in situ* high-pressure Brillouin spectroscopy in a diamond-anvil cell, we have determined the pressure dependence of acoustic velocities, adiabatic elastic moduli, bulk modulus, elastic anisotropy, and Cauchy violation of single-crystal methane hydrate (MH) at pressures up to 0.6 GPa and 296 K. Acoustic velocities show nearly isotropic behaviors with respect to the crystal orientation, and the slight TA-mode softening with pressure implies that the structure of MH is becoming less stable against the shear component under high pressures. Elastic moduli and bulk modulus indicate that MH is slightly more compressible than ice I_h. These results would help to investigate their mechanical and thermodynamical stabilities, and provide important constraints on the icy moons of the outer solar system.

Methane hydrate (MH) is an icelike compound, and shows hydrogen-bonded networks of water molecules that form rigid host cages in which CH_4 guest molecules are contained by van der Waals forces. MH (ideally $CH_4 \cdot 5.75H_2O$) (Ref. 1) is an important prototype for clathrate hydrates, and becomes an important material with respect to both a substantial future energy resource and a powerful greenhouse gas contributing to global warming.[1] The acoustic properties of MH and their expression are principally important to identify MH deposits and to estimate the hydrate concentration in the deep sea by using the bottom simulating reflection method,[2] and other elastic properties such as elastic moduli, bulk modulus, elastic anisotropy, and Cauchy violation are essential data to understand mechanical and thermodynamical stabilities of the MH guest-host system under various conditions.[1,3] Since the physical and thermochemical properties of clathrate hydrates are generally believed to be strongly similar in many ways to those of the most common ice I_h, it is also important to investigate the difference in the elastic properties between MH and ice I_h by considering their structure difference and an effect of CH_4 guest molecules.

At present, three gas-hydrate structures are well known:[1] the cubic structures I (*s*I) and II (*s*II), and the hexagonal structure *s*H. The *s*I structure is the most common form of clathrate hydrates in natural settings where methane is the main hydrate-forming gas. This structure consists of eight hydrogen-bonded water cages per unit cell, each containing one CH_4 guest molecule. Two types of cages are present in *s*I; two small 5^{12} cages (formed by 12 pentagons) and six large $5^{12}6^2$ cages (formed by 12 pentagons and two hexagons). Recently, high-pressure x-ray and Raman studies have been carried out to investigate the phase stability and transformation, and the cage occupancy in a single phase or polycrystalline MH prepared into a diamond-anvil cell (DAC).[4–9] Loveday *et al.*[6] and Shimizu *et al.*[8] showed that the cubic *s*I phase of MH is stable up to about $P = 0.9 \sim 1$ GPa at room temperature.

A few studies had been made for acoustic velocities[10,11] and elastic moduli[12] of MH. The theoretical prediction of longitudinal acoustic (LA) velocity in an *s*I phase of MH was carried out by Whalley.[10] In 1985, Kiefte *et al.*[11] measured LA velocities of eight kinds of *s*I and *s*II clathrate hydrates at low temperatures by using Brillouin spectroscopy. They described that the MH results are by far the most uncertain because of the very poor optical quality of the MH sample. However, they indicated that LA velocities can vary by about 20%, depending on composition and occupancy ratio.[13] Recently, Shpakov *et al.*[12] calculated the temperature dependence of adiabatic and isothermal elastic moduli by using a lattice-dynamics calculation. They presented that adiabatic elastic moduli of occupied MH show the larger values than its hypothetical empty lattice of MH.

In this paper, we present results of *in situ* Brillouin scattering in a single-crystal methane hydrate at pressures up to 0.6 GPa and room temperature, and determine the pressure dependence of acoustic velocities (v), adiabatic elastic moduli (C_{11}, C_{12}, and C_{44}), bulk modulus (B_S), elastic anisotropy [$A = 2C_{44}/(C_{11} - C_{12})$], and Cauchy violation ($\delta = C_{12} - C_{44} - 2P$). By comparing these results with water and ice I_h, we investigate the characteristics of elastic properties of methane hydrate under high pressures.

In our present high-pressure Brillouin studies we prepared successfully a pure MH single crystal into a small and thin sample chamber (diameter 0.4 mm, depth 0.04 mm) of a DAC: After mounting the DAC in which pure water is loaded in a pressure vessel, the air in its vessel was replaced by pure methane gas, and the chamber of the stainless-steel 301 gasket was filled with a droplet of pure water and compressed CH_4 gas. A single-crystal of MH was grown by increasing the pressure on a seed crystal, which coexists with water containing CH_4 at about 0.02 GPa and 296 K. In Fig. 1 one can see a MH single-crystal surrounded by water at about $P = 0.02$ GPa and $T = 296$ K. This observed *P-T* condition is consistent with the *P-T* phase relation determined by Dyadin *et al.*[14] The shape of a single-crystal MH is sometimes influenced by diamond anvils, i.e., by the touching of a MH crystal and the diamond culet faces. It has been confirmed from our visual observation and Raman studies that this crystal belongs to cubic *s*I and is stable up to $P = 0.9$ GPa at room temperature;[8] Raman spectra of CH_4 molecules are characterized by their cage occupancy in *s*I.
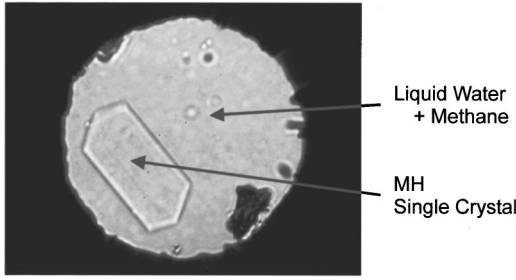
FIG. 1. Photomicrograph of single-crystal methane hydrate (MH) grown at about $P = 0.02$ GPa and 296 K in a sample chamber of a DAC, about 0.4 mm in diameter. This crystal of MH in the sI phase is in almost fully contact with both the upper and lower diamond culet faces, and is surrounded by water containing CH_4.

The pressure was measured by the ruby-scale method. The ruby was illuminated by the 514.5-nm line of an argon-ion laser with its intensities of less than 1 mW to prevent heating of the chip.[15] We also used the unified method of curve fitting for the ruby fluorescence peaks to avoid the disturbance by another signals. The pressure accuracy in this experiment is estimated to be about ± 0.02 GPa.

To determine the elastic properties of a single crystal MH we applied *in situ* high-pressure Brillouin spectroscopy with a tandem Fabry-Perot interferometer:[16,17] A complete mapping of the LA and transverse acoustic (TA) velocities in the various crystal directions and the full set of adiabatic elastic moduli can be exactly determined with *in situ* identification of the (unknown) crystal orientation at each pressure by analyzing the measured direction (angular) dependence of LA and TA velocities. As the excitation source, the 514.5-nm line (λ_0) of the argon-ion laser operated with single mode was used with an input power less than 40 mW. The Brillouin spectra were measured at $60°$ scattering geometry;[17] the Brillouin frequency shift ($\Delta \nu$) is related to the acoustic velocity (v) as $\Delta \nu_{60} = v_{60}/\lambda_0$. The thin sample chamber, where a MH crystal is in almost fully contact with both the upper and lower diamond culet faces, keeps the wave vector of the observed acoustic phonon parallel to the diamond culet faces, and enables us to avoid the detection of signals from water surrounding the MH crystal.

A typical Brillouin spectrum of MH at about $P = 0.02$ GPa and 296 K is shown in Fig. 2. The peaks of LA and TA modes are clearly observed. The signal from TA (shear) modes looks like one peak, whereas two peaks are usually expected to appear, except for the cases of (1) nearly elastic isotropy ($A \simeq 1$ as discussed below), i.e., the close frequencies of two shear modes; (2) the weak intensity for one of their peaks; and (3) the phonon wave vector along the $\langle 100 \rangle$ or $\langle 111 \rangle$ direction in a cubic system. Therefore, only one peak for TA modes is probably due to high elastic isotropy and/or the weak intensity of TA peak. At $60°$ scattering geometry, we measured Brillouin frequency shifts (i.e., acoustic velocities) in $10°$ intervals of rotation angle about the load axis of the DAC at each pressure. Acoustic velocities of LA and TA modes show slight but significant angular dependences for the analysis in our *in situ* Brillouin method;[16,17] The computerized least-squares fit was applied to determine
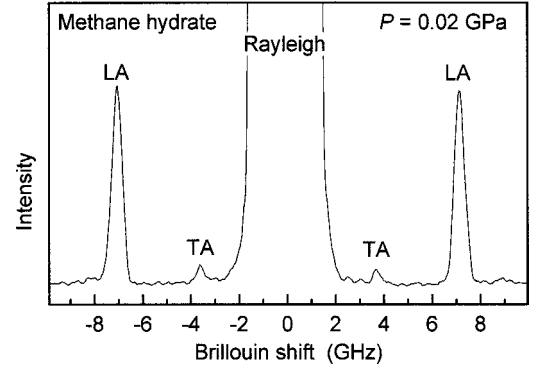

FIG. 2. Brillouin spectrum of single-crystal methane hydrate (MH) at about $P = 0.02$ GPa and room temperature, and at $60°$ scattering geometry. LA and TA are Brillouin-shifted signals from longitudinal and transverse acoustic waves, respectively.

three elastic moduli and single-crystal orientation simultaneously, by using the Brillouin equation $v_j = f_j(C_{11}/\rho, C_{12}/\rho, C_{44}/\rho, \theta, \phi, \chi)$. The typical results are $C_{11}/\rho = 13.2$, $C_{12}/\rho = 7.07$, and $C_{44}/\rho = 3.76$ km^2/s^2 at about $P = 0.02$ GPa and 296 K.

In Figs. 3(a) and 3(b), the MH acoustic velocities of the sI phase are shown, respectively, for typical $\langle 100 \rangle$ and $\langle 110 \rangle$ directions as a function of pressure up to 0.6 GPa at room temperature; $v_{LA-100} = (C_{11}/\rho)^{1/2}$, $v_{TA1-100} = v_{TA2-100} = (C_{44}/\rho)^{1/2}$, $v_{LA-110} = [(C_{11}+C_{12}+2C_{44})/(2\rho)]^{1/2}$, $v_{TA1-110} = [(C_{11}-C_{12})/(2\rho)]^{1/2}$, and $v_{TA2-110} = (C_{44}/\rho)^{1/2}$, where ρ is the density and v_{TA1} and v_{TA2} are slow and fast TA velocities, respectively. The velocities of TA$_1$ and TA$_2$ modes along the $\langle 110 \rangle$ direction are found to be well resolved by using our analyzed C_{ij}/ρ on an *in situ* high-pressure Brillouin method.[16,17] With increasing pressure
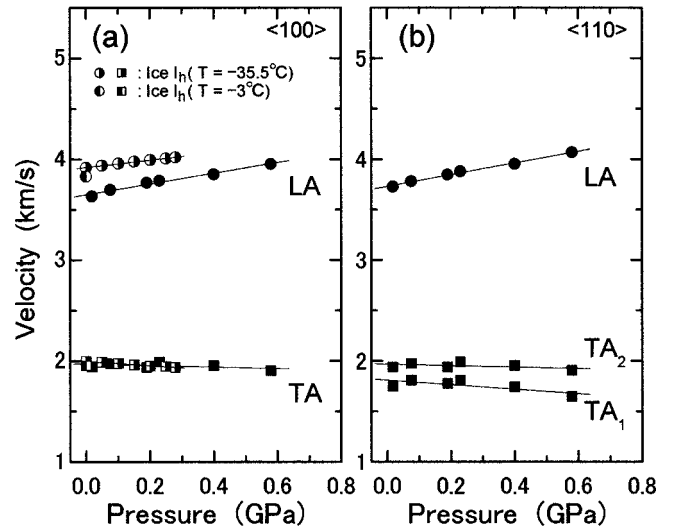

FIG. 3. Pressure dependence of LA and TA velocities of single-crystal methane hydrate indicated by solid symbols for (a) the $\langle 100 \rangle$ direction and (b) the $\langle 110 \rangle$ direction up to $P = 0.6$ GPa and at room temperature. Average LA and TA velocities of ice (I_h) (Ref. 18) are plotted in (a) up to $P = 0.28$ GPa at -35.5 °C, and $P = 1$ atm at -3 °C for comparison.
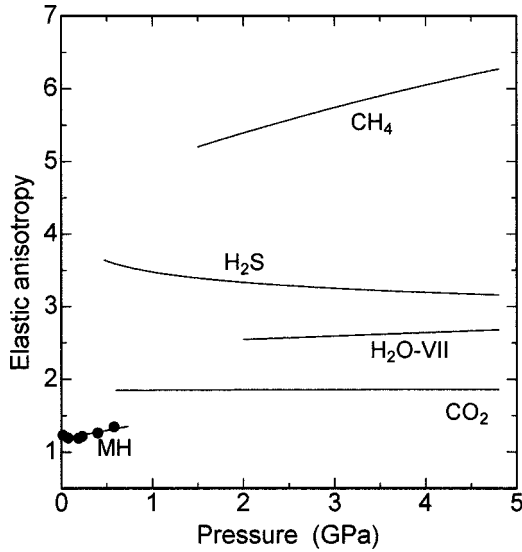
FIG. 4. Pressure dependence of the elastic anisotropy $[A = 2C_{44}/(C_{11}-C_{12})]$ of methane hydrate (MH, solid circles). Typical data of pressure-induced cubic molecular-solids (Ref. 20) are shown by solid lines for comparison.

FIG. 5. Pressure dependence of adiabatic elastic moduli (C_{ij}) and bulk modulus (B_S) of methane hydrate up to $P=0.6$ GPa at room temperature for the cases of 100% (solid lines and solid symbols) and 75% (dotted lines and open symbols) cage occupancies.

LA velocities show the increase, but TA velocities decrease gradually. These behaviors of TA velocities indicate that the MH becomes gradually less stable with respect to the shear component at higher pressures. To investigate the difference in acoustic velocities (due to their structure difference) between the present MH and ice I_h, we show Gagnon et al.'s average velocities[18] of LA and TA modes at pressures up to 0.28 GPa and $T = -35.5\,°C$ [see Fig. 3(a)]. The shear TA velocities of MH and ice I_h show almost the same values, but the compressional LA velocities of MH show a significant difference from those of ice I_h. Even if we consider one data point of LA and TA velocities at $-3\,°C$ near the melting point [see Fig. 3(a)],[18] the differences in LA velocity are expected to be more than 7% at the investigated pressure region. As for water, its velocity shows about 2 km/s at $P = 0.02$ GPa range;[19] therefore, the presence of MH strongly affects acoustic velocities in the deep sea.

Although cubic crystals are optically isotropic, they usually exhibit substantial elastic anisotropy (A) which is defined as $A = (v_{TA2-110}/v_{TA1-110})^2 = 2C_{44}/(C_{11}-C_{12})$. For isotropic elasticity ($A=1$), two shear velocities $v_{TA2-110}$ and $v_{TA1-110}$ are equal and degenerate. Figure 3(b) shows a small difference between $v_{TA2-110}$ and $v_{TA1-110}$, which resulted in $A=1.23$ at about $P=0.02$ GPa and 296 K, and a slight increase to about $A=1.34$ at $P=0.6$ GPa, as shown in Fig. 4. This result of nearly isotropic behavior reveals the reason only one TA peak is usually observed for an arbitrarily oriented MH crystal in the DAC. This nearly isotropic elasticity is noted to be a specific feature of MH, in contrast to typical data of pressure-induced cubic molecular solids (CO_2, H_2O-VII, H_2S, and CH_4), showing between $A=2$ and 6 at high pressures.[20] These elastic properties seem to be due to the structural features of MH: (1) the void-rich arrangement of hydrogen-bonded networks which are widespread to almost all directions in order to contain cages, and
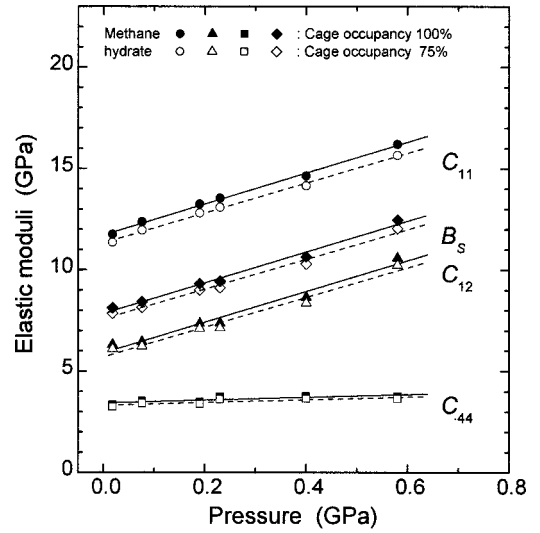
(2) the larger departures from regularity, i.e., larger deviations from the ideal angular geometry in a tetrahedral coordination of oxygen atoms (these deviations are necessary in order to form a MH structure in contrast to ice I_h).[21]

Hirai et al.[4] determined the pressure dependence of a lattice constant of MH by x-ray diffraction measurements at room temperature. From their results we calculated the pressure dependence of density ρ for 100% and 75% cage occupancies; for 100% cage occupancy, for example, the ρ values increase from about 0.9 to 1.0 g/cm³ with pressure up to 0.43 GPa, and above this pressure the ρ just becomes larger than 1.0 g/cm³. These results and our velocity data yielded a determination of the adiabatic elastic moduli of C_{11}, C_{12}, and C_{44} as functions of pressure. The solid and dotted lines in Fig. 5 indicate the results of C_{ij} under assumptions of cage occupancies of 100% and 75%, respectively. Since both small and large cages in the sI phase of MH are known to be almost occupied by CH_4 molecules,[21] it is becoming clear that the actual elastic moduli are most likely to take values between solid and dotted lines. The theoretical calculations[12] of $C_{11}=12.8$ and $C_{44}=3.6$ GPa at $P=1$ atm and 270 K are in good agreement with the present experimental results. The adiabatic bulk modulus $B_S[=(C_{11}+2C_{12})/3]$ is also presented in Fig. 5. C_{11} and C_{12} of MH increase almost linearly with pressure, but C_{44} remains almost constant, an effect associated with the slight softening behaviors of TA velocities with pressure. Their pressure dependence are estimated as $dC_{11}/dP=7.64$, $dC_{12}/dP=7.59$, $dC_{44}/dP=0.69$, and $dB_S/dP=7.61$ for the case of 100% cage occupancy. It is worthwhile to compare the present results with those of ice I_h (Ref. 18) for the investigation of their effect through the structure difference.[21] The difference between MH and ice I_h is found on compressional C_{11} and C_{33} components; MH shows about 20% smaller values. These results indicate that MH is significantly more compressible than ice I_h, that is, about 10% as compressible as estimated from their B_S data

for the case of 100% cage occupancy. This compressible feature of MH is expected to be dominated by the void-rich structure of the host cage.[22] Therefore, the considerable difference in compressional components of elastic moduli between MH and ice I_h can be accounted for by their structural difference; MH is more void-rich and open than the hexagonal puckered ice I_h.

The high-pressure Cauchy relation for hydrostatic conditions[17,23] $C_{12} = C_{44} + 2P$ is satisfied when interatomic forces are purely central. The deviation $\delta (= C_{12} - C_{44} - 2P)$ is caused by effects due to many-body forces in a solid. The magnitude of the present experimental δ shows about 2.5 GPa at about $P = 0.02$ GPa, and increases almost linearly to $\delta = 5.5$ GPa at $P = 0.6$ GPa with increasing pressure. This notable result of the Cauchy violation shows that the noncentral nature of the bonding becomes greater at higher pressures, which suggests an important role of increasing interaction among host water molecules through their strengthening hydrogen bonds at higher pressures.

In summary, *in situ* high-pressure Brillouin measurements of the single-crystal methane hydrate have provided complete studies of acoustic velocities, adiabatic elastic moduli, the bulk modulus, the elastic anisotropy, and the Cauchy violation up to $P = 0.6$ GPa and 296 K. Many different properties among methane hydrate, water, and ice I_h were presented, which can offer useful information to many fields relating to the research of gas hydrates and to many regions relating to the outer solar system permitting mixtures of water and various gases to crystallize into icy solids.[24]

[1] E. D. Sloan, *Clathrate Hydrates of Natural Gases*, 2nd ed. (Dekker, New York, 1998).

[2] W. S. Holbrook, H. Hoskins, W. T. Wood, R. A. Stephen, and D. Lizarralde, Science **273**, 1840 (1996).

[3] B. A. Buffett, Annu. Rev. Earth Planet Sci. **28**, 477 (2000).

[4] H. Hirai, T. Kondo, M. Hasegawa, T. Yagi, Y. Yamamoto, T. Komai, K. Nagashima, M. Sakashita, H. Fujihisa, and K. Aoki, J. Phys. Chem. B **104**, 1429 (2000).

[5] I. M. Chou, A. Sharma, R. C. Burruss, J. Shu, H. K. Mao, R. J. Hemley, A. F. Goncharov, L. A. Stern, and S. H. Kirby, Proc. Natl. Acad. Sci. U.S.A. **97**, 13 484 (2000).

[6] J. S. Loveday, R. J. Nelmes, M. Guthrie, S. A. Belmonte, D. R. Allan, D. D. Klug, J. S. Tse, and Y. P. Handa, Nature (London) **410**, 661 (2001).

[7] I. M. Chou, A. Sharma, R. C. Burruss, R. J. Hemley, A. F. Goncharov, L. A. Stern, and S. H. Kirby, J. Phys. Chem. A **105**, 4664 (2001).

[8] H. Shimizu, T. Kumazaki, T. Kume, and S. Sasaki, J. Phys. Chem. B **106**, 30 (2002).

[9] H. Hirai, Y. Uchihara, H. Fujihisa, M. Sakashita, E. Katoh, K. Aoki, K. Nagashima, Y. Yamamoto, and T. Yagi, J. Chem. Phys. **115**, 7066 (2001).

[10] E. Whalley, J. Geophys. Res. **85**, 2539 (1980).

[11] H. Kiefte, M. J. Clouter, and R. E. Gagnon, J. Phys. Chem. **89**, 3103 (1985).

[12] V. P. Shpakov, J. S. Tse, C. A. Tulk, B. Kvamme, and V. R. Belosludov, Chem. Phys. Lett. **282**, 107 (1998).

[13] C. F. Pearson, P. M. Halleck, P. L. McGulre, R. Hermes, and M. Mathews, J. Phys. Chem. **87**, 4180 (1983).

[14] Y. A. Dyadin, E. Y. Aladko, and E. G. Larionov, Mendeleev Commun. **7**, 34 (1997).

[15] H. T. Lotz and J. A. Schouten, J. Chem. Phys. **111**, 10 242 (1999).

[16] H. Shimizu and S. Sasaki, Science **257**, 514 (1992).

[17] H. Shimizu, H. Tashiro, T. Kume, and S. Sasaki, Phys. Rev. Lett. **86**, 4568 (2001).

[18] R. E. Gagnon, H. Kiefte, M. J. Clouter, and E. Whalley, J. Chem. Phys. **89**, 4522 (1988).

[19] H. Shimizu, Rev. High Pressure Sci. Technol. **7**, 1124 (1998).

[20] H. Shimizu, K. Kamabuchi, T. Kume, and S. Sasaki, Phys. Rev. B **59**, 11 727 (1999).

[21] C. Gutt, B. Asmussen, W. Press, M. R. Johnson, Y. P. Handa, and J. S. Tse, J. Chem. Phys. **113**, 4713 (2000).

[22] The cage occupancy can be also responsible for the compressibility, but until now its significant change with pressure has not been confirmed in the sI phase of methane hydrate.

[23] M. Grimsditch, P. Loubeyre, and A. Polian, Phys. Rev. B **33**, 7192 (1986).

[24] W. Durham and L. Stern, Annu. Rev. Earth Planet Sci. **29**, 295 (2001).